Machine learning approaches to assess fouling on field samples

L. Krause, L. Vogler, K. Nolte, J. Koc, Axel Rosenhahn
Analytical Chemistry – Biointerfaces, Ruhr-University Bochum

Collaborators

FLORIDA TECH
H. Gardner
A. Wassick
K. Richard
K. Hunsucker
G.W. Swain

USNA UNITED STATES NAVAL ACADEMY
M. Schultz

Leibniz Universität Hannover
B. Rosenhahn

Antifouling conference Gothenburg, Sweden 2025

ONR Revolutionary Research . . . Relevant Results

Assessment of Fouling release coatings

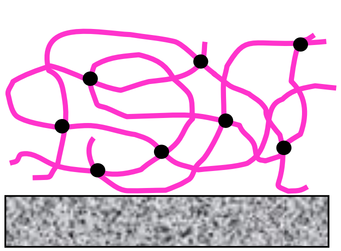

Low-fouling polymer

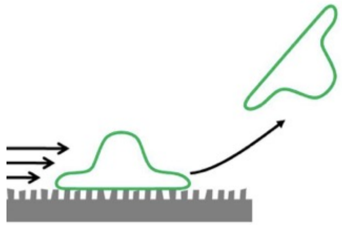

Fouling-release

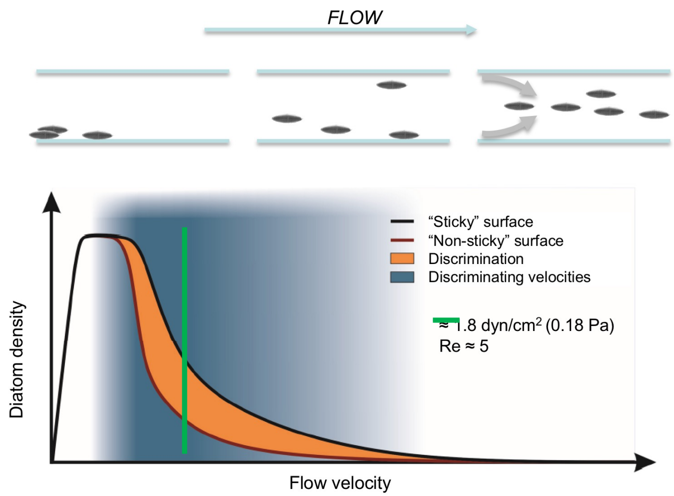

Dynamic accumulation under flow as predictor for fouling release potential

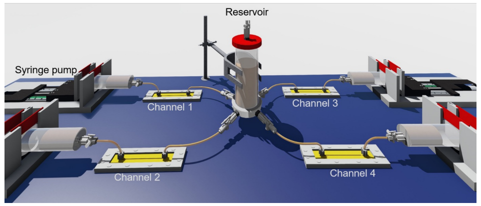

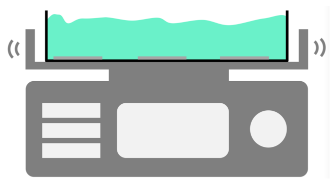

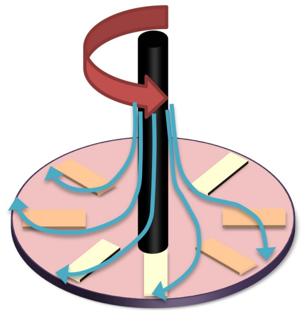

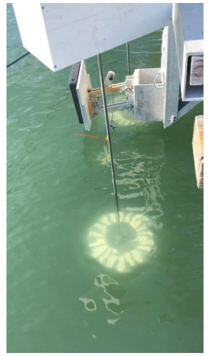

FLORIDA TECH USNA

Arpa-Sancet, Christophis, Rosenhahn, Biointerphases 2012, 7, 26
Alles, Rosenhahn, Biofouling 2015, 31(5), 469
Nolte, Schwarze, Rosenhahn, Biofouling 2017, 33(7), 531
Nolte, Schwarze, Beyer, Özcan, Rosenhahn, Biointerphases 2018, 13(4), 041007
Nolte, Koc, Barros, Hunsucker, Schultz, Swain, Rosenhahn, Biofouling 2018, 34(4), 398

Analysis of field data

- Counting of diatoms in microfluics works automatically (particle detection)
- Counting of field slides requires manpower as objects on surface are heterogeneous
- Initial DDT/HUDT/EG6 dataset: 4 repl x 9 chem x 60 fov = 2160 Fields of view
- Time for man. analysis per field of view: 5-10 min (depending on coverage, 16 MPix image)
  => 2160 x 7 min = 252 h of counting (30 days by first and second semester students)
- To be analyzed in 2018/2019: >600 slides, (>36000 FOV ≈ 525 days of counting)

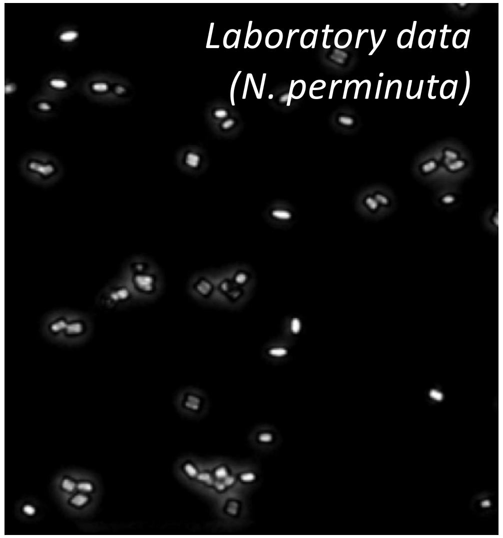

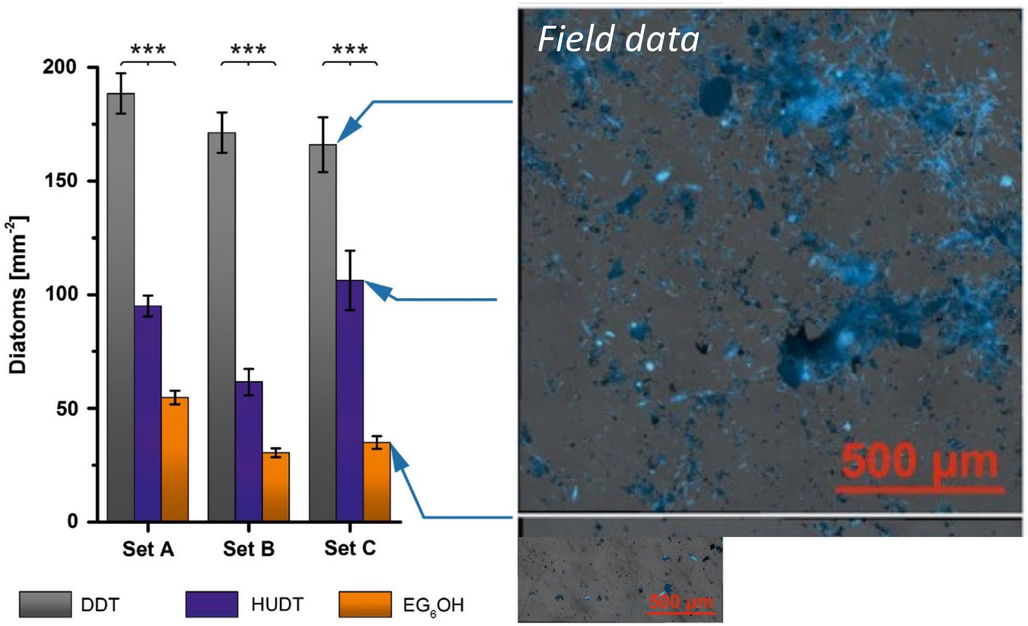

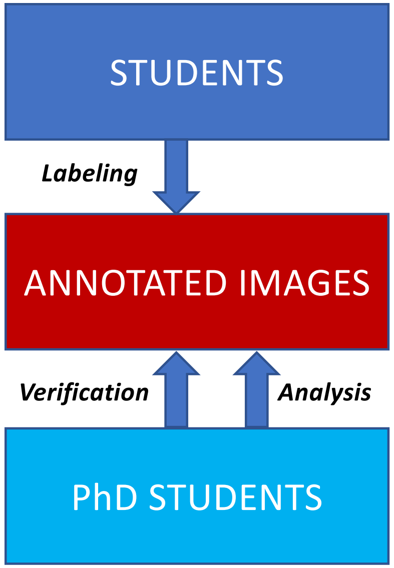

Nolte, Koc, Barros, Hunsucker, Schultz, Swain, Rosenhahn, Biofouling 2018, 34, 398

Deep learning neuronal network

Challenge similar to automated driving

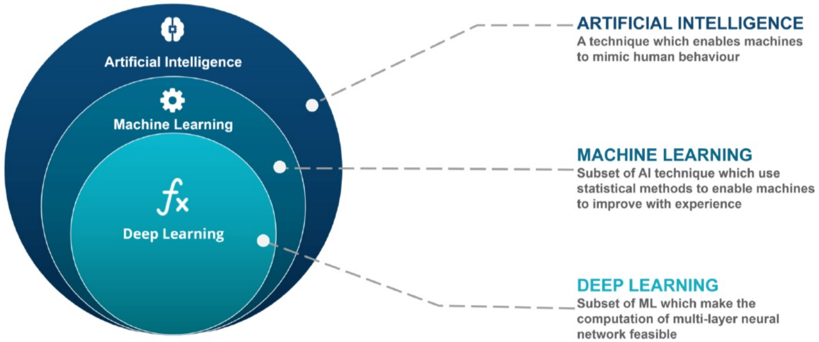

Reduction of free parameters
(less parameters -> faster analysis)

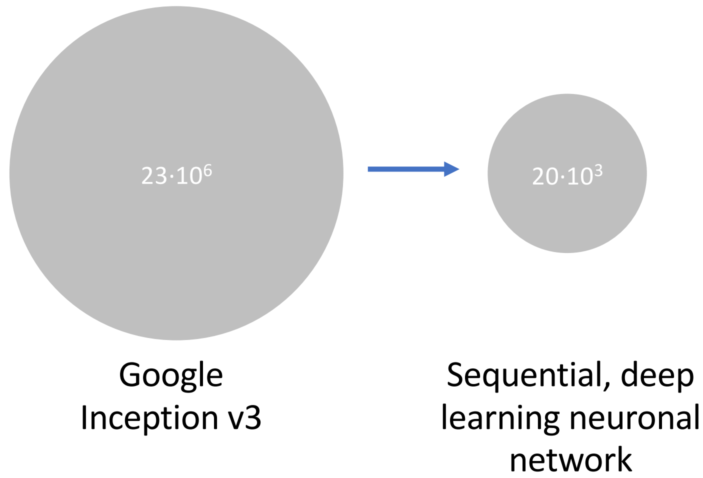

- Goal : Counting diatoms on field samples with particulates and other artifacts present
- Binary classifier -> Not only detection of presence of an object (yes/no) but probability for occurrence in a specified region
- Runs entirely on graphic cards
- Fast analysis (≈1s per image)

Collaboration with B. Rosenhahn, Institute for Information Technology, Leibniz-University Hannover

Learning dataset

Microscopy data and learning sets

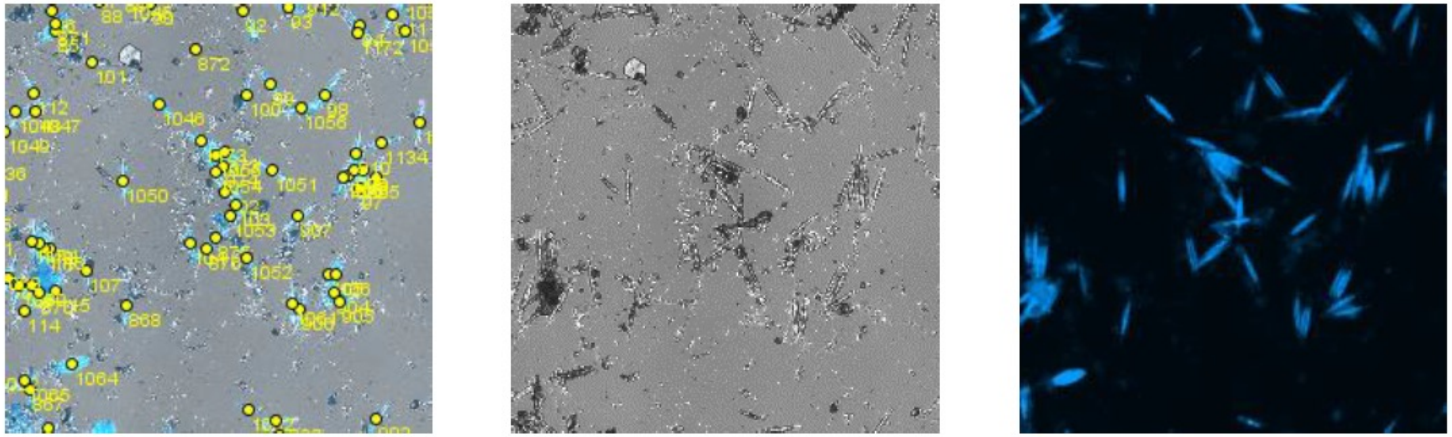

Coordinates **Phase Contrast** **Fluorescence**

Learning dataset :

- Initial labeling could not be used due to inaccurate labels (edge of diatom or even next to diatom in close vicinity)
- Diatom positions assigned by different users (different accuracy, required careful selection)
- Expert relabeling with markers in the center of the diatoms were necessary
- Data augumentation (Contrast, brightness, mirroring, rotation)

Krause, Koc, Rosenhahn, Rosenhahn, Envir. Sci. Technol. 2020, 54(16), 10022

Counting of field data with deep learning

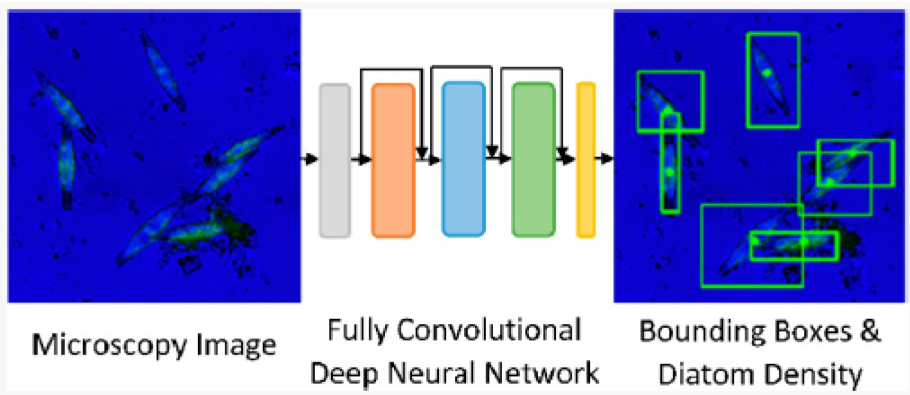

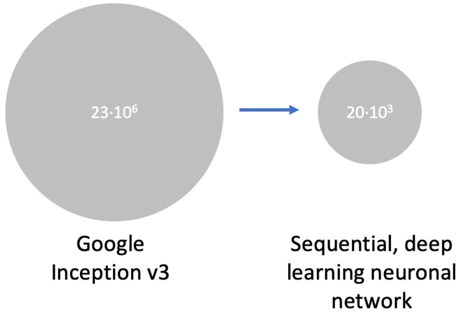

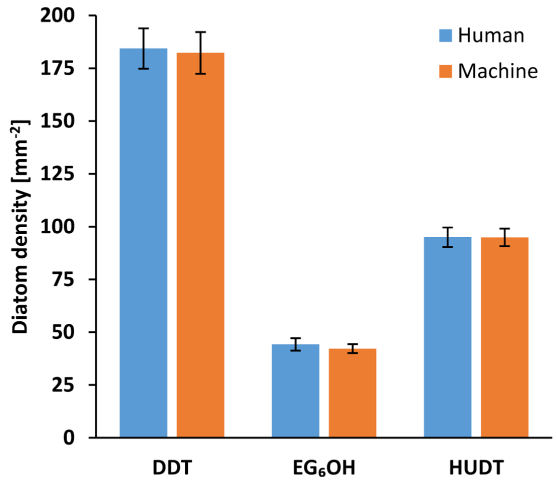

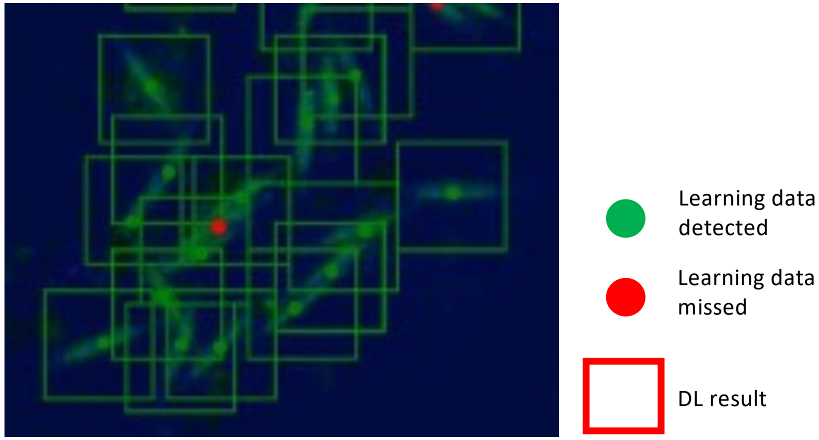

- Deep learning counts as good as humans
- Human counting depends on person

- Time required for 600 images was 8 minutes (0.8 s/image) (would take 70 h by human) and DL works non-supervised!

Krause, Koc, Rosenhahn, Rosenhahn, Envir. Sci. Technol. 2020, 54(16), 10022

From image recognition to semantic segmentation

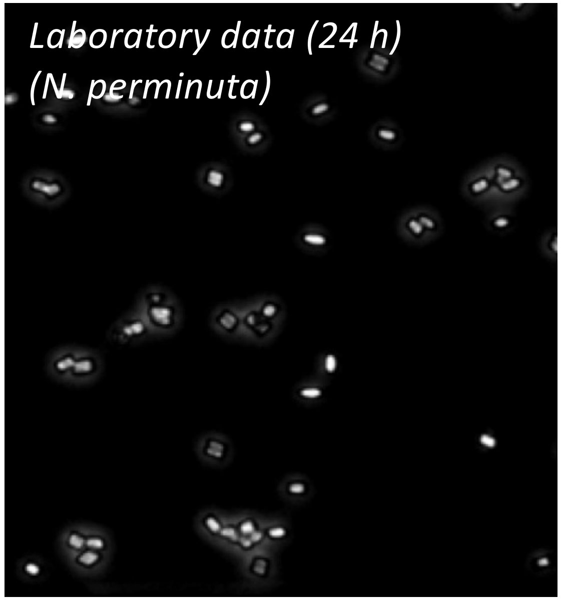

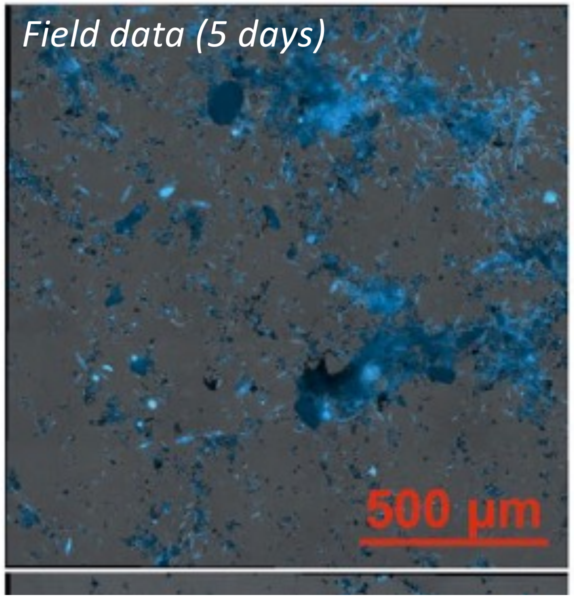

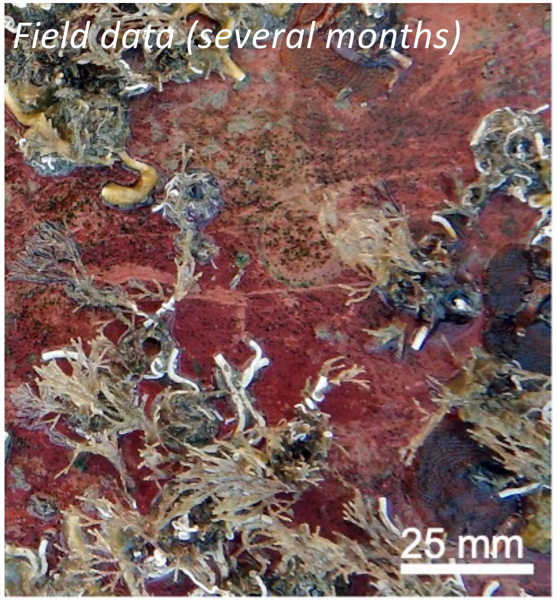

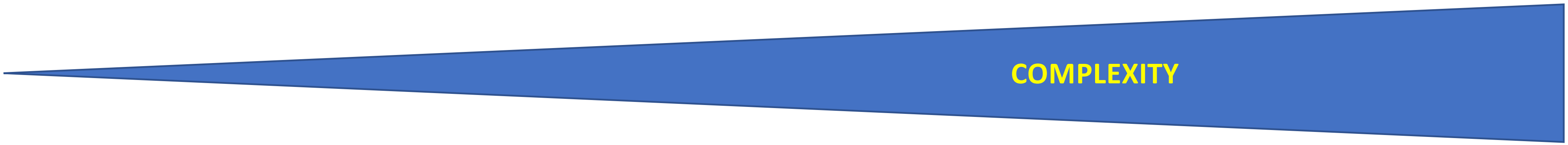

Visual assessment and CCPe Annotation

ASTM D6990-20

Standard Practice for Evaluating Biofouling Resistance and Physical Performance of Marine Coating Systems

Significance and Use

5.1 This practice is designed to provide guidance to a panel inspector for quantitative and consistent evaluation of coating performance from test panels coated with marine antifouling coating systems. The practice assesses performance of coating systems based on both antifouling and physical properties.

5.2 The user is cautioned that the results are representative for the specific region and time of year in which the specimens are immersed. It shall be noted that interpretation of results will depend on the geographical location where the test is conducted, whether the coated specimens are exposed either totally or partially immersed, under static or dynamic conditions, and position and orientation.

5.3 Simultaneous testing of a proven standard antifouling coating system (known to minimize fouling accumulation, for example, containing biocide or active agent(s) to prevent fouling settlement/growth) in the specific marine environment shall be included as a reference to assist in interpretation of results. In addition, a negative control (inert surface susceptible to heavy fouling) shall be included on a regular basis. For the exposure to be valid, the surface of the negative control should show heavy fouling relative to the standard system(s).

5.4 Marine coating systems that produce positive results relevant to the standard system(s) show potential for use in protecting underwater marine structures.

5.5 The format can be utilized independent of exposure protocol and coating type, and provides the end user with a consistent practice and format for reporting of performance rating.

- Quantitative and consistent visual evaluation of coatings
- Appropriate consideration of positive and negative controls
- Method should work for a broad range of coating types

ELSEVIER Computers & Geosciences 32 (2006) 1259–1269
www.elsevier.com/locate/cageo

Coral Point Count with Excel extensions (CPCe): A Visual Basic program for the determination of coral and substrate coverage using random point count methodology ☆

Kevin E. Kohler*, Shaun M. Gill

National Coral Reef Institute, Nova Southeastern University Oceanographic Center, Dania Beach, FL 33004, USA

Received 19 July 2005; received in revised form 17 November 2005; accepted 21 November 2005

Occurrence based (random point annotation)

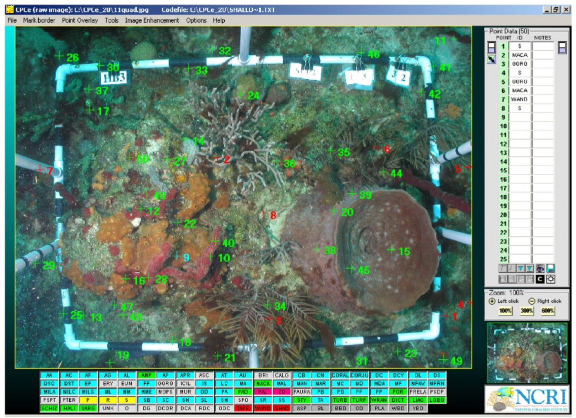

Area based (manual segmentation)

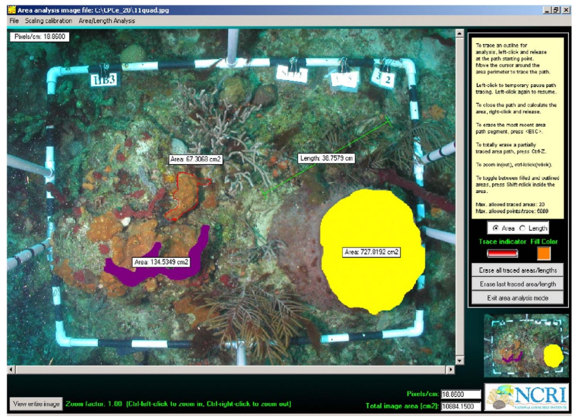

From image recognition to semantic segmentation

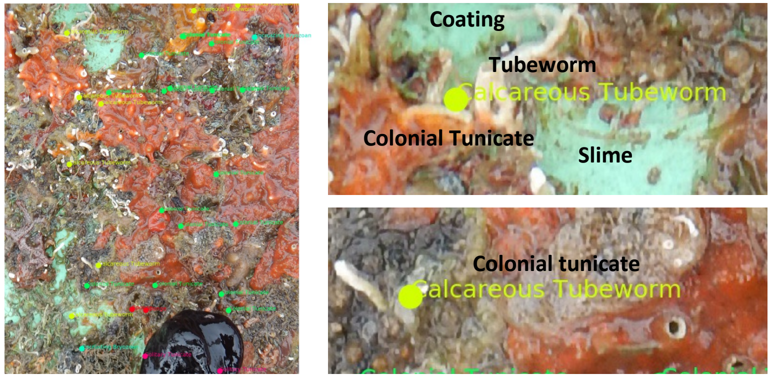

FLORIDA TECH

Data base from FIT : 486 panel images
Point assignment according to CPCe (24300 data points)

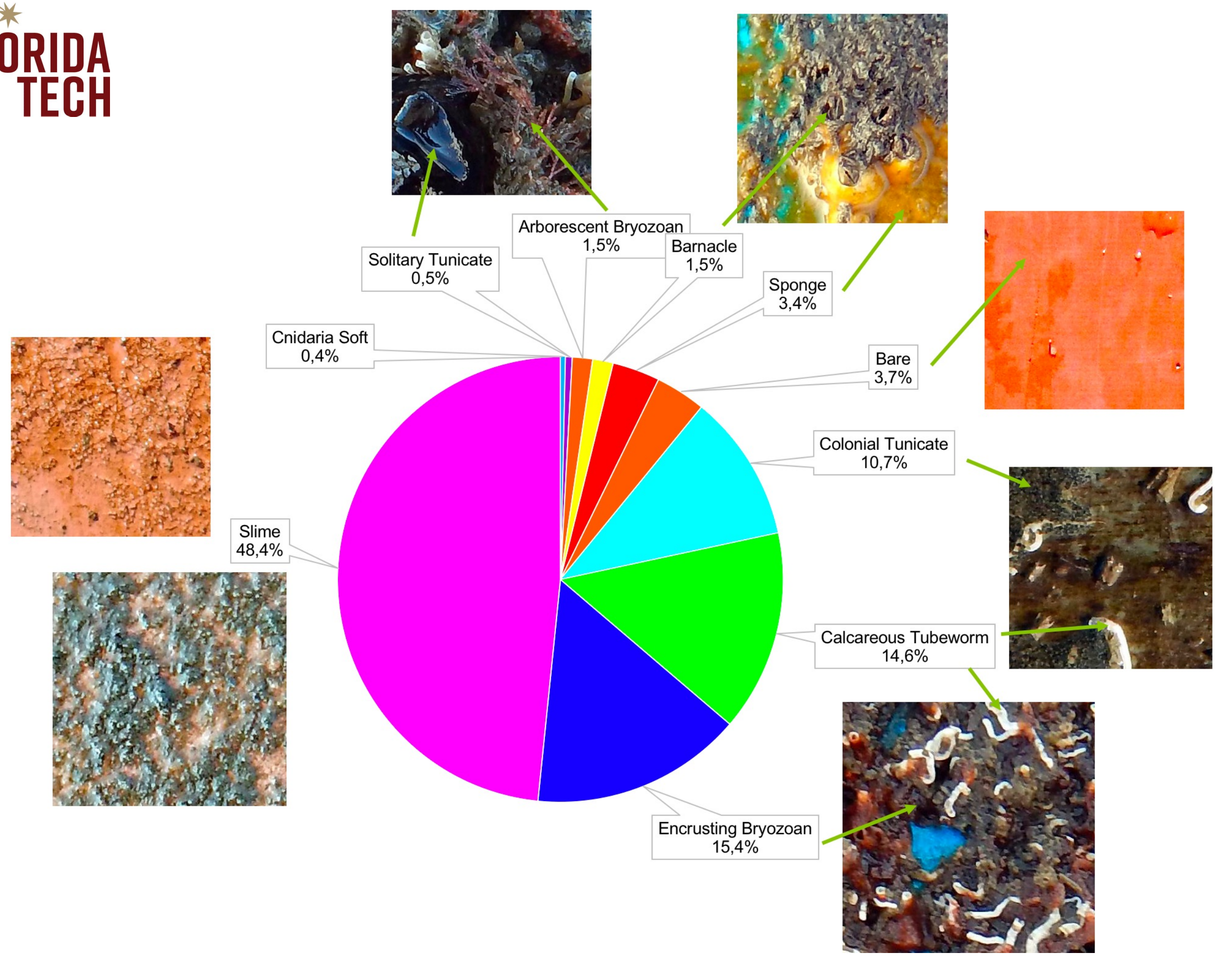

Challenges for automated image analysis

- Complex composition of fouling organisms
- Mixture of species at certain spots
- Vicinity of randomly chosen CPCe points can be heterogeneous
- Imbalanced panel depending species distribution

L. Krause, E. Manderfeld, P. Gnutt, L. Vogler, A. Wassick, K. Richard, M. Rudolph, K. Hunsucker, G. Swain, B. Rosenhahn, A. Rosenhahn, Biofouling 2023, 39(1), 64

Unet architecture for semantic segmentation

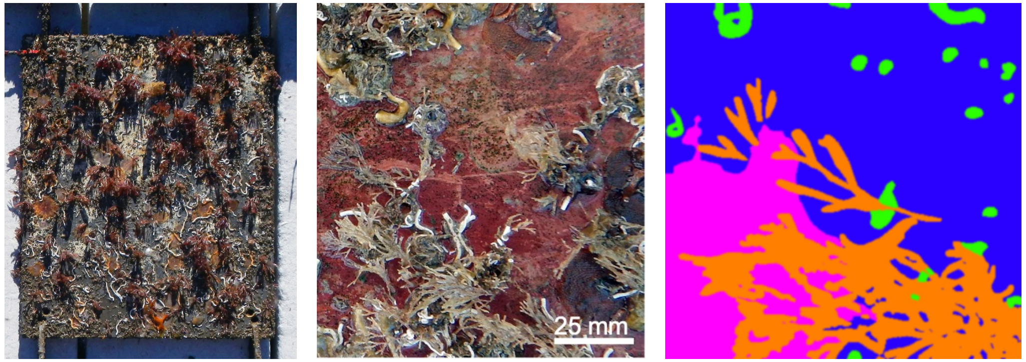

- Not only object detection and counting but semantic segmentation
- Labeling of entire panels is time demanding and induces a species imbalance
- Separated Panel into patches of ≈5% of the total panel size
- ≈300 randomly chosen fully manually segmented images (13 fully manually segmented panels)

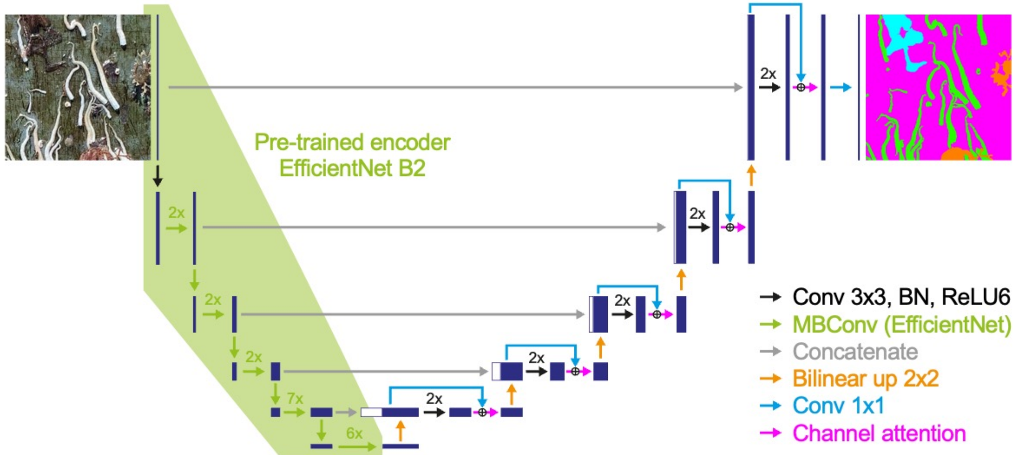

Supplementary Figure 5: Final model architecture. A pre-trained EfficientNet B2 encoder is deployed for the contraction path of the U-Net. Arrows denote operations and rectangles represent the resulting tensor. Crossing of arrows represents element-wise addition.

Table 1: Performance of adapted U-Net model architectures. Results for image tiles from validation set. Best performing configurations for a metric are highlighted.

Configuration	Accuracy	IoU	F1	Precision	Recall
U-Net (baseline)	0.959	0.614	0.746	0.758	0.739
+ Pretrained EfficientNet encoder	0.974	0.735	0.841	0.842	**0.841**
+ Residual decoder links	**0.976**	0.747	**0.849**	**0.864**	0.836
+ Channel attention & rebalanced decoder filters	**0.976**	**0.749**	**0.849**	0.861	0.840

L. Krause, E. Manderfeld, P. Gnutt, L. Vogler, A. Wassick, K. Richard, M. Rudolph, K. Hunsucker, G. Swain, B. Rosenhahn, A. Rosenhahn, Biofouling 2023, 39(1), 64

Manually segmented ground truth data

Status in the middle of the project

- Intersection over union (IOU) of 0.3 for 10 classes
- ≈300 training images BUT high class imbalance
- Architecture optimization and additional labeling of previously unlabeled regions/tiles of high entropy (e.g. bare versus slime as bare is underrepresented)

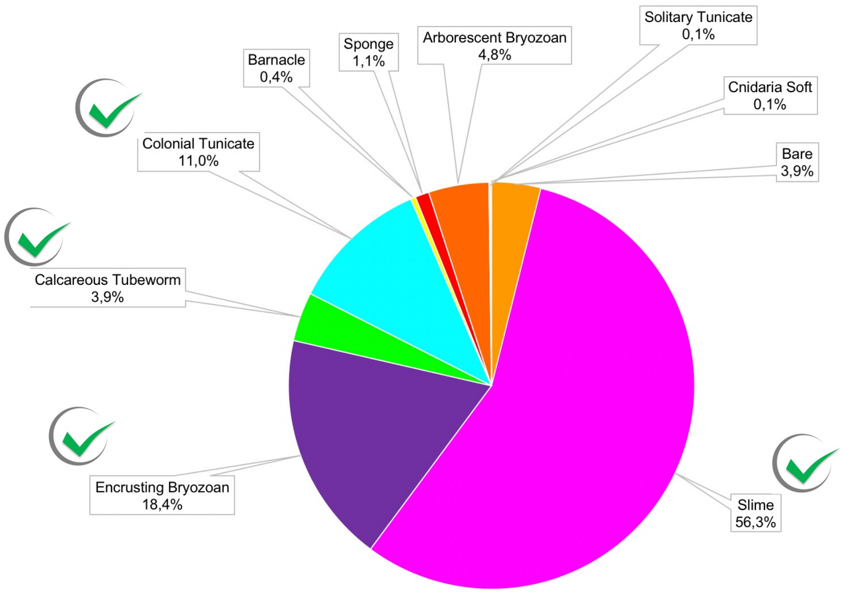

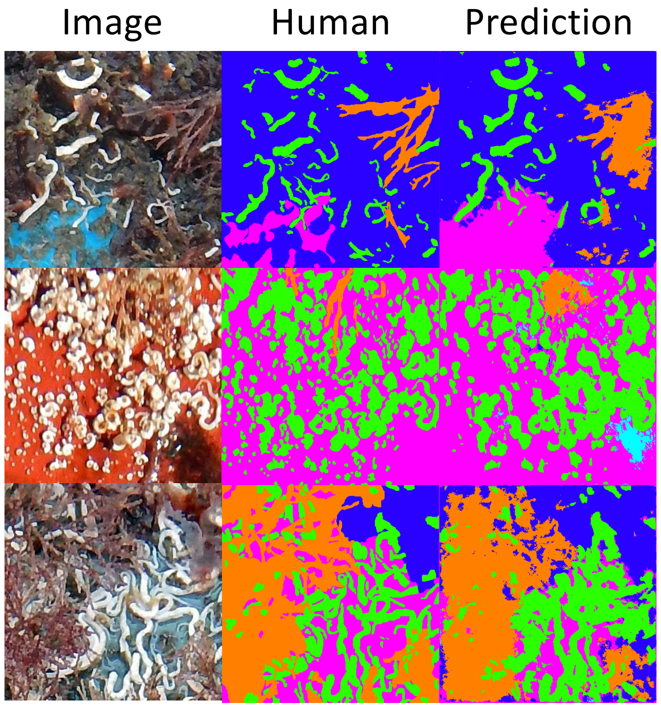

L. Krause, E. Manderfeld, P. Gnutt, L. Vogler, A. Wassick, K. Richard, M. Rudolph, K. Hunsucker, G. Swain, B. Rosenhahn, A. Rosenhahn, Biofouling 2023, 39(1), 64

Segmentation performance

Supplementary Table 2: Segmentation performance of the enhanced U-Net. Metrics are reported as the class-wise mean of image tiles from the validation set. Best values (≥ 85 %) are highlighted.

Class	Bare	Slime	Encrusting Bryozoan	Calcareous Tubeworm	Colonial Tunicate	Barnacle	Sponge	Arborescent Bryozoan	Solitary Tunicate	Cnidaria	Mean
Accuracy	**0.986**	**0.911**	**0.978**	**0.981**	**0.969**	**0.976**	**0.988**	**0.982**	**0.999**	**0.993**	0.976
IoU	**0.908**	0.807	0.772	0.644	0.667	0.666	0.879	0.505	**0.966**	0.672	0.749
F1	**0.952**	**0.893**	**0.872**	0.784	0.800	0.800	**0.936**	0.671	**0.983**	0.804	0.849
Precision	**0.932**	**0.885**	**0.861**	0.805	**0.862**	0.801	**0.926**	0.709	**0.974**	**0.858**	0.861
Recall	**0.973**	**0.901**	**0.882**	0.764	0.747	0.799	**0.946**	0.637	**0.991**	0.756	0.840

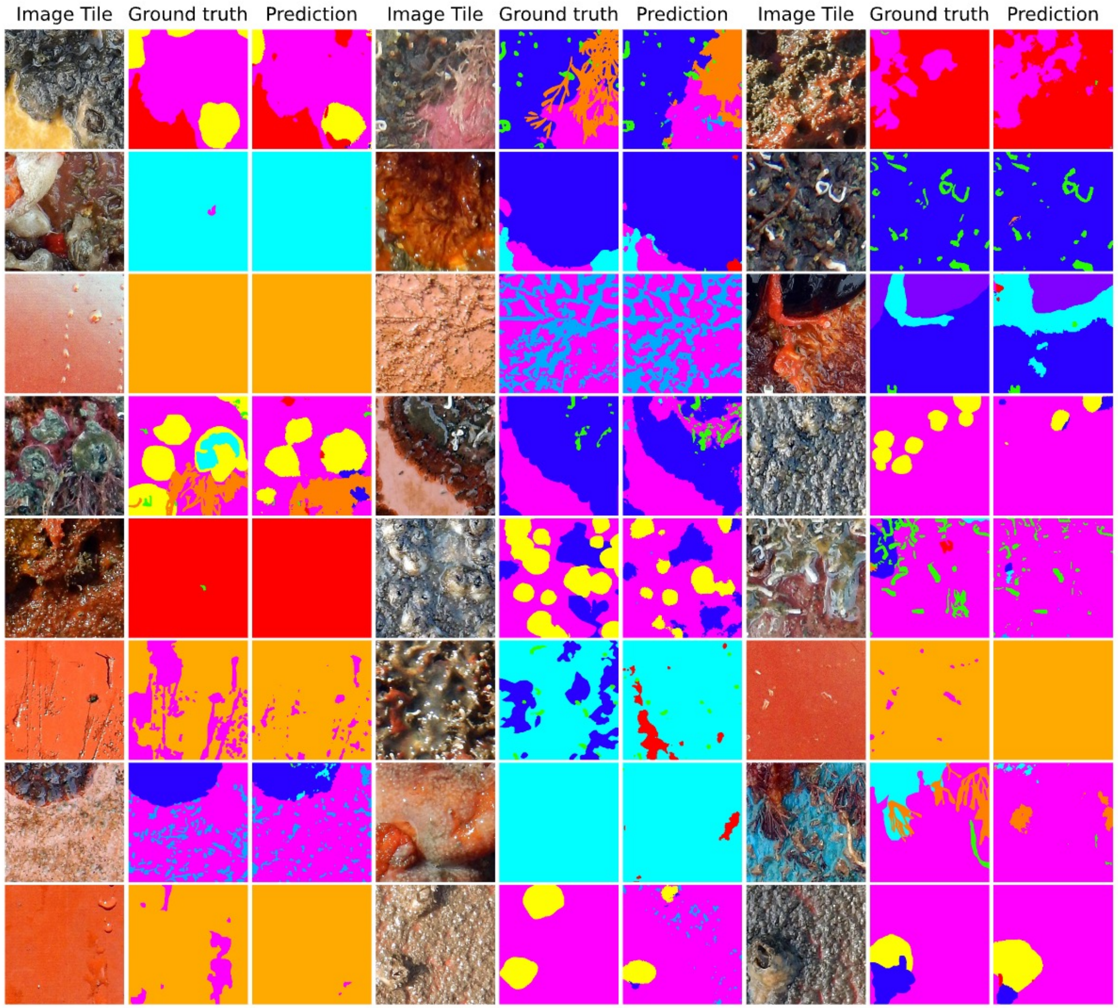

L. Krause, E. Manderfeld, P. Gnutt, L. Vogler, A. Wassick, K. Richard, M. Rudolph, K. Hunsucker, G. Swain, B. Rosenhahn, A. Rosenhahn, Biofouling 2023, 39(1), 64

Semantic segmentation of fouling in the field

t-SNE (t-distributed stochastic neighbor embedding) of the high-level features extracted by the encoder path of U-Net

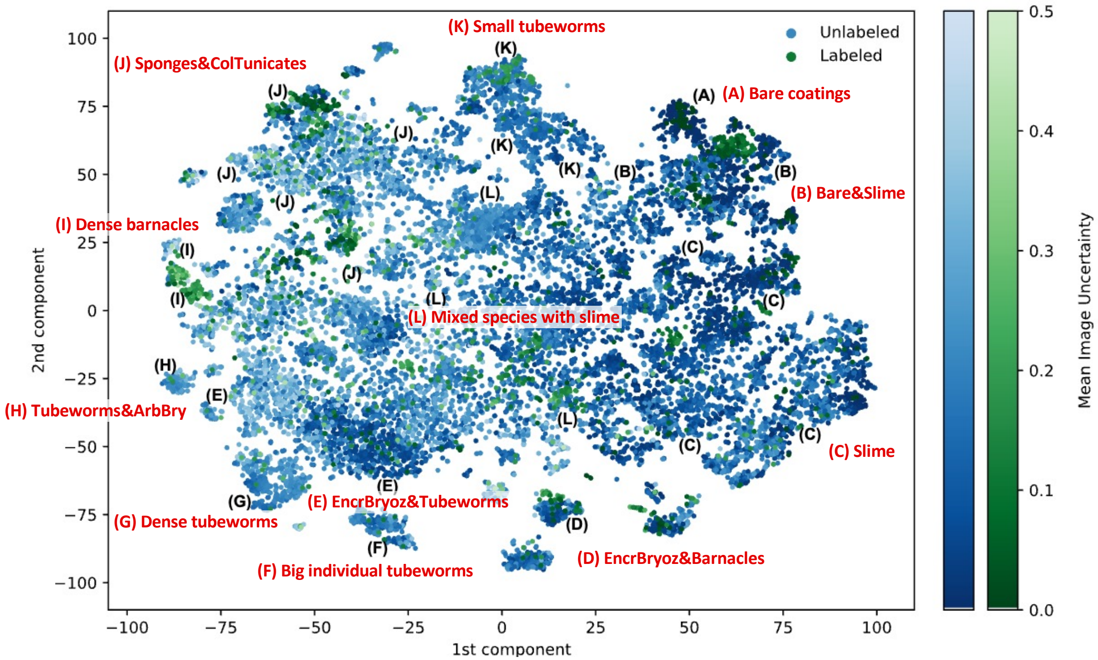

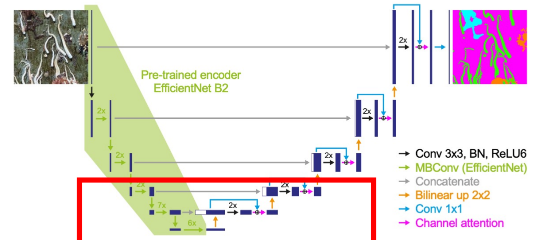

Supplementary Figure 5: Final model architecture. A pre-trained EfficientNet B2 encoder is deployed for the contraction path of the U-Net. Arrows denote operations and rectangles represent the resulting tensor. Crossing of arrows represents element-wise addition.

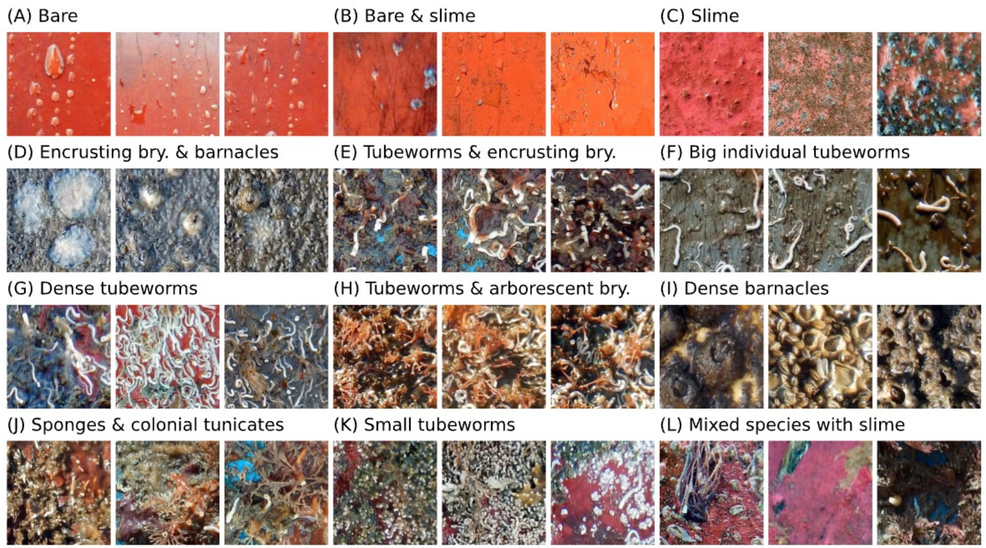

L. Krause, E. Manderfeld, P. Gnutt, L. Vogler, A. Wassick, K. Richard, M. Rudolph, K. Hunsucker, G. Swain, B. Rosenhahn, A. Rosenhahn, Biofouling 2023, 39(1), 64

Estimation of sampling error in CPCe annotation

Supplementary Table 1: Error of random point annotation. The class-wise random point annotation error was quantified by the mean absolute error (MAE), the mean absolute percentage error (MAPE), and the left-out probability (LOP). Metrics were obtained by uniform sampling of $\boldsymbol{n} = \mathbf{50}$ random points with segmentation masks from manual annotation and $\boldsymbol{N} = \mathbf{1000}$ repetitions per image. All values are given as percentage. Reported uncertainties refer to the standard error.

Class	Bare	Slime	Encrusting Bryozoan	Calcareous Tubeworm	Colonial Tunicate	Barnacle	Sponge	Arborescent Bryozoan	Solitary Tunicate	Cnidaria
MAE	3.94 ± 0.02	3.72 ± 0.01	2.58 ± 0.01	1.55 ± 0.03	2.83 ± 0.01	4.74 ± 0.00	2.17 ± 0.01	2.17 ± 0.01	4.12 ± 0.01	4.40 ± 0.00
MAPE	5.7 ± 0.0	48.0 ± 0.4	72.9 ± 0.4	113.6 ± 0.5	67.3 ± 0.4	20.1 ± 0.0	60.0 ± 0.5	88.1 ± 0.5	33.6 ± 0.2	24.4 ± 0.0
LOP	0.0 ± 0.0	17.4 ± 0.2	27.9 ± 0.3	53.7 ± 0.3	30.0 ± 0.2	0.0 ± 0.0	23.4 ± 0.2	38.4 ± 0.3	6.2 ± 0.1	0.0 ± 0.0

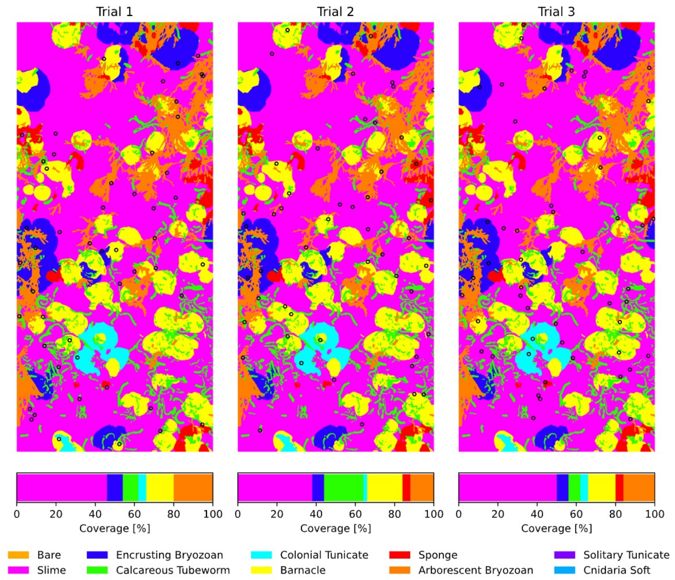

- Fully segmented panel image was used to ”simulate” CPCe sampling accuracy
- While frequently occurring species that cover larger areas like bare substrate, barnacles, slime or tunicates has lower left-out probabilities, small objects like tubeworms have a high leaving out probability

L. Krause, E. Manderfeld, P. Gnutt, L. Vogler, A. Wassick, K. Richard, M. Rudolph, K. Hunsucker, G. Swain, B. Rosenhahn, A. Rosenhahn, Biofouling 2023, 39(1), 64

Fouling progression analysis

FLORIDA TECH

Criticizm on the method: Bias for top surface layer, but fouling organisms with surface contact relevant

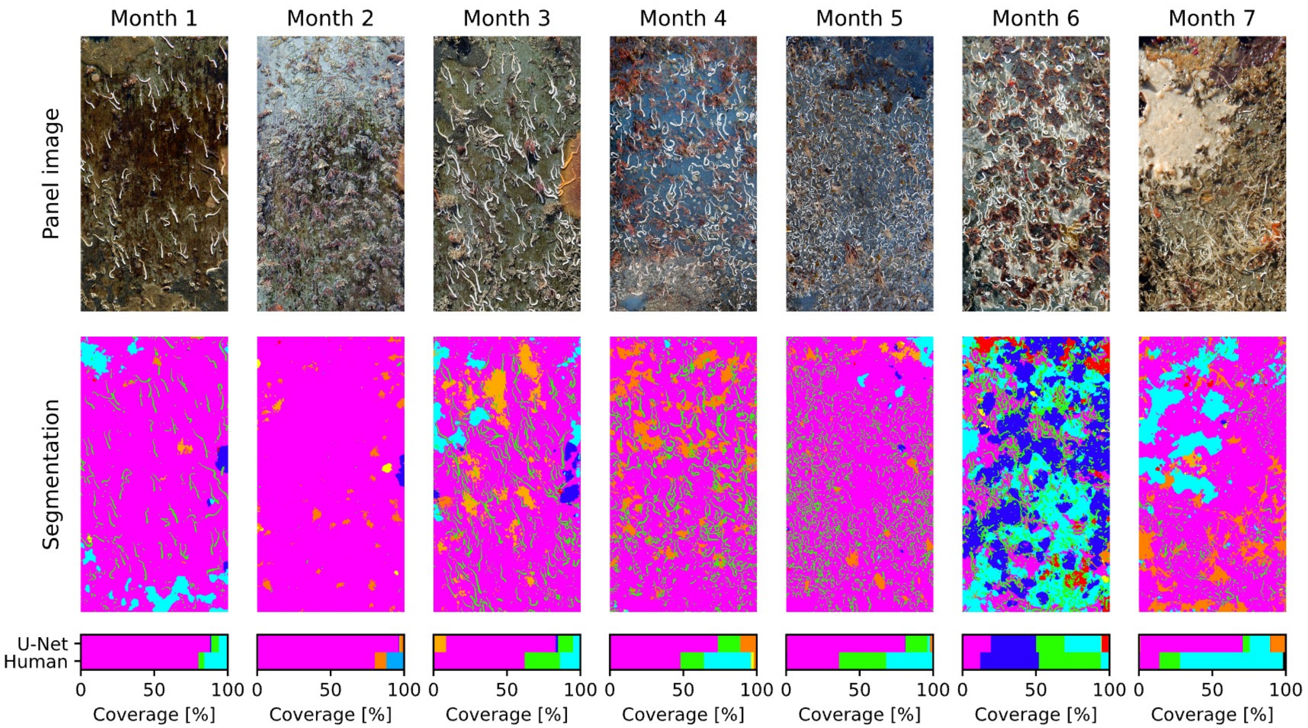

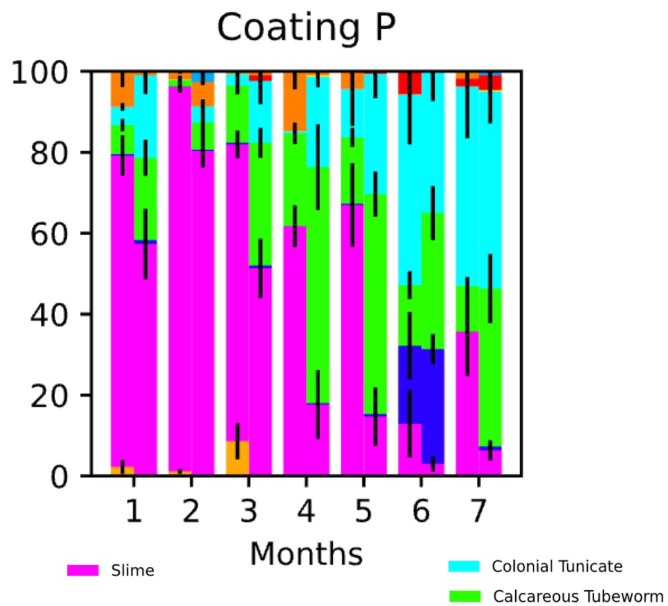

Coverage by organisms is changing over time

Bars: *left* U-Net, *right* human

Bare, Slime, Encrusting Bryozoan, Calcareous Tubeworm, Colonial Tunicate, Barnacle, Sponge, Arborescent Bryozoan, Solitary Tunicate, Cnidaria Soft, Others

L. Krause, E. Manderfeld, P. Gnutt, L. Vogler, A. Wassick, K. Richard, M. Rudolph, K. Hunsucker, G. Swain, B. Rosenhahn, A. Rosenhahn, Biofouling 2023, 39(1), 64

Point resolved fouling progression analysis

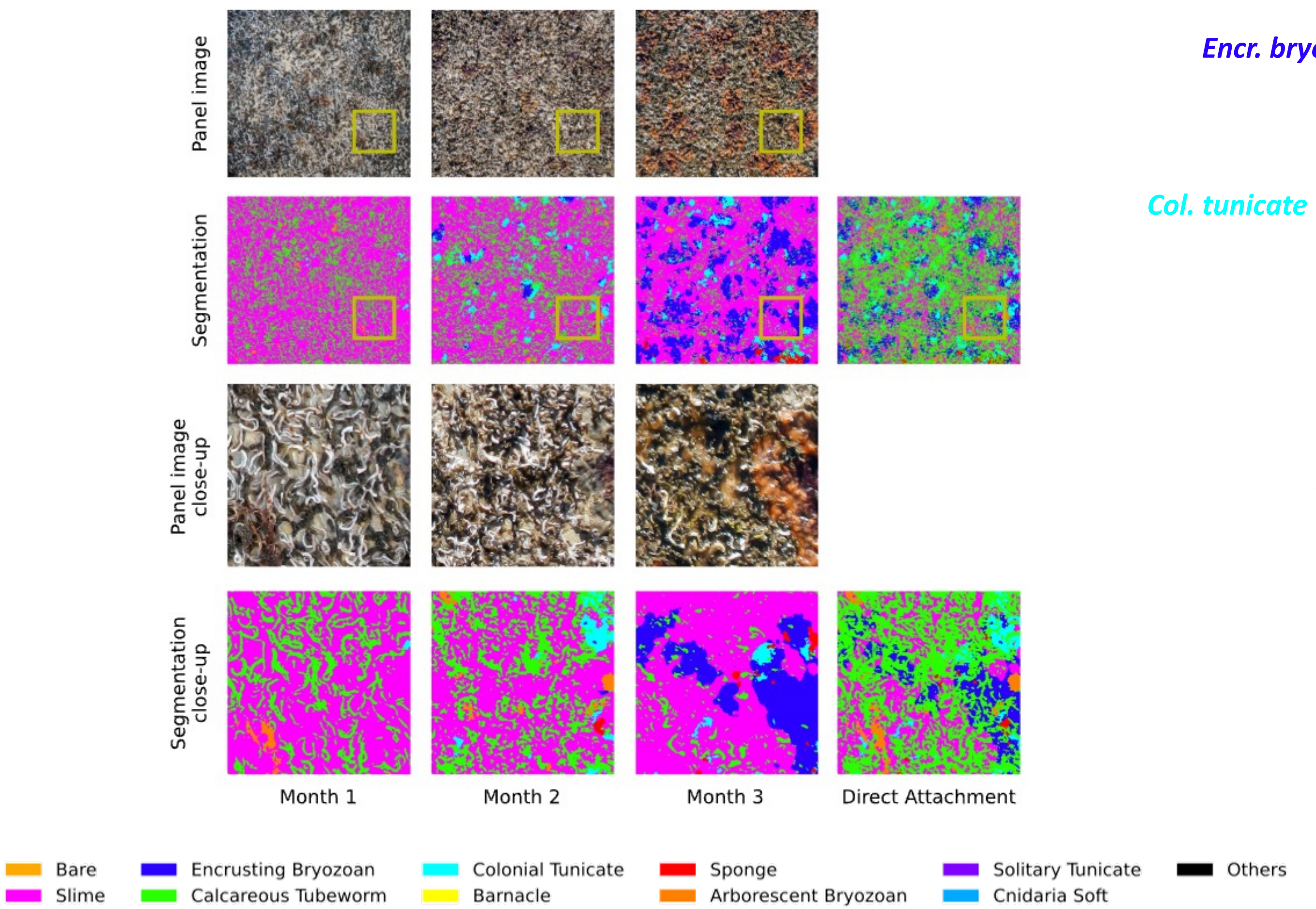

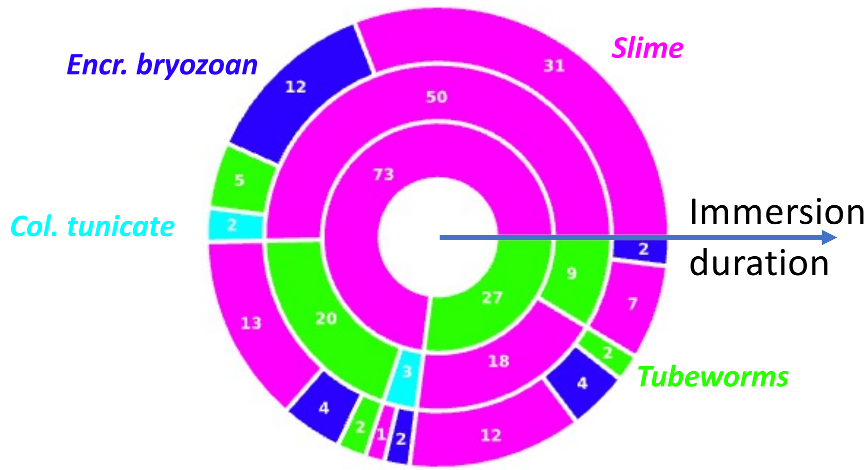

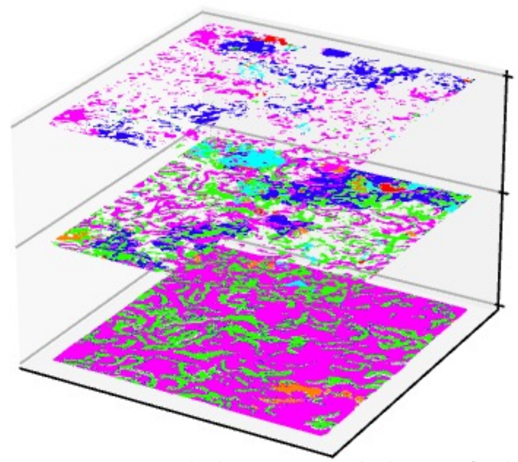

L. Krause, E. Manderfeld, P. Gnutt, L. Vogler, A. Wassick, K. Richard, M. Rudolph, K. Hunsucker, G. Swain, B. Rosenhahn, A. Rosenhahn, Biofouling 2023, 39(1), 64

Summary

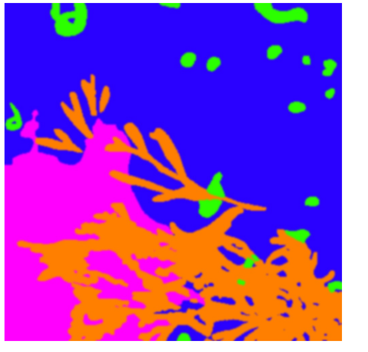

- Very **early fouling** dominated e.g. by diatoms can be analyzed by image detection using a binary classifier
- Labeling and analysis of **fouling communities** on surfaces can be accomplished by semantic segmentation with deep learning

Challenges

- Semantic segmentation has a **bias towards the top layer** of fouling. Analysis of time series can help.
- Many of the larger species (e.g. solitary tunicates, arborescent bryozoans) **collapse** if the panels are retrieved from water. Is the assessment accurate? (Similar question applies to CPCe method and to a lesser degree to for ASTM assessment). Does the analysis of underwater (diver) images help?
- If multiple species are grown **symbiotically as new entity**, how should such cases be analyzed/interpreted?
- Need to define how can the data be **reduced** into “heavy fouling”, ”light fouling”, and “clean coatings”.

Advantages

- Once established, it may serve as fast and reliable method for fouling assessment with limited human bias

ICMCF 2026

International congress on marine corrosion and fouling
26.-31.7.26
Henry Ford Building, FU Berlin
Berlin Germany

Organizers:
T. Heusinger von Waldegge, D. Stübing
Fraunhofer IFAM, Bremen

with COIPM committe